Optical properties of lead borate glasses containing Dy^{3+} ions

Joanna Pisarska

Department of Materials Science, Silesian University of Technology, Krasińskiego 8,
40-019 Katowice, Poland

E-mail: Joanna.Pisarska@polsl.pl

Abstract
Optical properties of lead borate glasses containing Dy^{3+} ions were examined using absorption
and luminescence measurements and theoretical calculations based on the Judd–Ofelt
framework and the Inokuti–Hirayama model. The luminescence spectra show two characteristic
bands at 480 and 573 nm, which are due to $^4F_{9/2}$–$^6H_{15/2}$ (blue) and $^4F_{9/2}$–$^6H_{13/2}$ (yellow)
transitions of trivalent Dy^{3+} ions. The yellow/blue luminescence and its decay were analyzed as
a function of activator concentration.

1. Introduction

During the past decades, rare earth and/or transition metal
containing heavy metal lead glasses based on PbO–XO$_2$
(X = Ge [1], Si [2] or Te [3]), PbO–Y$_2$O$_3$ (Y = Bi and/or
Ga [4–8]) and PbO–Z$_2$O$_5$ (Z = P [9] or Nb [10]) have been
extensively studied using optical spectroscopy. Of these, PbO–
B$_2$O$_3$ based glasses are attractive optical materials due to their
unique structural and physicochemical properties [11–13].
Depending on PbO/B$_2$O$_3$ ratios, various borate groups like
penta- and di-borates containing three and/or four coordinated
boron, ring- and chain-type metaborate units containing non-
bridging oxygen atoms, and boroxol rings can be found in lead
borate glass systems. The presence of structurally different
borate units in the B$_2$O$_3$–PbO glass network is favorable for
investigation using spectroscopic methods. These structural
differences are usually correlated to chemical composition,
kinds of modifiers and conditions during glass manufacturing.
Moreover, PbO–B$_2$O$_3$ based glasses are characterized by
second-order optical nonlinearity [14, 15] and wider visible-
to-NIR transparency range in comparison to traditional borate
glasses. Refractive indices varying from 1.6 to 1.9 [16] and
forward/back BO$_3$ $\leftrightarrow$ BO$_4$ conversion [17] strongly depend
on the B$_2$O$_3$/PbO ratio in the glass composition.

On the other hand, lead borate glass creates an excellent
host to incorporate rare earth ions. The role of PbO and rare
earth ions in the structure, conductivity, dielectric and optical
properties of lead borate based glasses has been extensively
discussed [18–22]. The luminescence properties of lead borate
glasses doped with Ln^{3+} ions have been examined in our

previously published works. The quite intense visible [17] and
near-infrared [23] luminescence spectra for selected rare earth
ions in B$_2$O$_3$–PbO based glasses were registered. However,
luminescence of Dy^{3+} was analyzed considerably less than
other Ln^{3+} ions.

Optical properties of Dy^{3+} ions in some crystals [24–34],
glasses [34–42] and glass-ceramics [43–46] are reported in
the literature. Low-phonon-energy glasses containing Dy^{3+}
ions have been studied for near-infrared (1.3 μm) optical
amplifiers [47–51] and yellow–green up-conversion [52–55]
applications. Special attention has been devoted to Dy-doped
borate glasses with various chemical compositions [56–61].

In the present study, the optical properties of Dy^{3+}
ions in B$_2$O$_3$–PbO–Al$_2$O$_3$–WO$_3$ glasses have been examined.
The systematic spectroscopic studies include absorption
and emission, Judd–Ofelt calculations and luminescence
decay analysis for glass samples with various activator
concentrations. Several spectroscopic parameters for Dy^{3+}
ions in lead borate glasses were evaluated. The experimental
results were compared to the theoretical calculations obtained
from the Judd–Ofelt framework [62, 63] and the Inokuti–
Hirayama model [64].

2. Synthesis and experimental methods

Series of lead borate glasses (in wt%), $(73 - x)$PbO–
18B$_2$O$_3$–6Al$_2$O$_3$–3WO$_3$–xDy$_2$O$_3$, were prepared by mixing
and melting of appropriate amounts of lead oxide, boron oxide,
aluminum oxide, tungsten oxide and dysprosium oxide of high
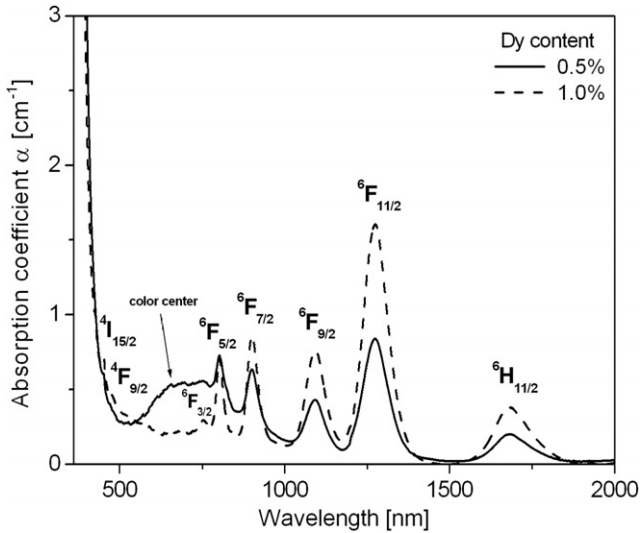purity (99.99%, Aldrich Chemical Co.). Reagents were mixed

Figure 1. Absorption spectra for Dy^{3+} ions in lead borate glasses.

homogeneously together in an agate ball mill for 2 h. In doped samples, the PbO was partially substituted by dysprosium ions in various concentrations ($x = 0.5$–3 wt%). Dy-doped lead borate glasses were melted at 900 °C for 1 h, quenched and annealed below T_g in order to eliminate the internal mechanical stresses.

Absorption spectra were recorded using a Varian 2300 UV–vis–NIR spectrophotometer. Luminescence spectra and decay curves were observed using a Jobin Yvon Fluoromax4 spectrophotometer. The spectral resolution was equal to 0.1 nm. Luminescence decay curves were detected with an accuracy of ± 1 μs. All spectral measurements were carried out at room temperature.

3. Results and discussion

3.1. Absorption and the Judd–Ofelt calculations

Selected room-temperature absorption spectra for Dy^{3+} ions (0.5 and 1 wt%) in lead borate glasses are presented in figure 1. The spectra consist of several inhomogeneously broadened transitions from the $^{6}H_{15/2}$ ground state to the $^{6}H_{11/2}$, $^{6}F_{11/2}$, $^{6}F_{9/2}$, $^{6}F_{7/2}$, $^{6}F_{5/2}$, $^{6}F_{3/2}$, $^{4}F_{9/2}$, $^{4}I_{15/2}$ and $^{4}G_{11/2}$ excited states belonging to the $4f^{9}$ electronic configuration of trivalent dysprosium. For the sample with low (0.5 wt%) Dy^{3+} concentration, a quite intense and broadened absorption band between 500 and 800 nm can be additionally observed, which is probably associated with the presence of a color center. The visual observation of glass samples proves this hypothesis. This glass sample has an intense green color in contrast to the other well prepared yellow Dy-doped lead borate glasses. The glass sample with 1.0 wt% Dy^{3+} was used for further Judd–Ofelt calculations.

The radiative transition probabilities for excited levels of Dy^{3+} ions have been calculated using the standard Judd–Ofelt theory [62, 63]. The spectral intensities of the absorption bands are estimated by measuring the areas under the absorption lines

using the relation

$$P_{meas} = 4.318 \times 10^{-9} \int \varepsilon(\nu) \, d\nu \qquad (1)$$

where $\int \varepsilon(\nu)$ represents the area under the absorption line. The molar absorptivity $\varepsilon(\nu)$ of the corresponding band at energy ν (cm^{-1}) under the integral is given by

$$\varepsilon(\nu) = A/c \cdot l \qquad (2)$$

where A indicates the absorbance, c is the concentration of the Dy^{3+} ion in mol l^{-1} and l is the optical path length.

The theoretical oscillator strength for each transition of Dy^{3+} ions, within $4f^{9}$ configuration, was calculated using the relation

$$P_{calc} = \frac{8\pi^{2}mc(n^{2}+2)^{2}}{3h\lambda(2J+1) \cdot 9n} \times \sum_{t=2,4,6} \Omega_{t}(\langle 4f^{N}J \| U^{t} \| 4f^{N}J' \rangle)^{2} \qquad (3)$$

where m is the mass of the electron, c is the velocity of light, h is the Planck constant and λ is the mean wavelength of the transition. In performing the analysis, a constant value of 1.92 was used for n, the refractive index of the medium. $\|U^{t}\|^{2}$ represents the square of the matrix elements of the unit tensor operator U^{t} connecting the initial and final states. The squared reduced matrix elements $\|U^{t}\|^{2}$ taken from [34] have been used for calculations. Equation (3) accounts for electric dipole line strengths only.

As mentioned above, the oscillator strengths of the observed transitions were obtained from the optical absorption bands, whereas the theoretical oscillator strengths were calculated based on the Judd–Ofelt theory using equation (3). Measured and calculated data are collected in table 1. The three Ω_{t} ($t = 2, 4, 6$) intensity parameters of equation (3) are found by a least squares fitting of the experimental and theoretical electric dipole oscillator strengths. The phenomenological Judd–Ofelt parameters for Dy^{3+} ions in lead borate glasses are found to be $\Omega_{2} = 4.90 \pm 0.18$, $\Omega_{4} = 0.94 \pm 0.19$, $\Omega_{6} = 2.07 \pm 0.09$ (in 10^{-20} cm^{2} units). The quality of the fit can be expressed using the following relation: $d = \Sigma(P_{meas} - P_{calc})$. The deviation of the fitted values is equal to $d = 0.7 \times 10^{-6}$. The Ω_{t} values are used to calculate the radiative transition probabilities, branching ratios and radiative lifetimes.

The radiative transition probability A_{J} for excited levels of Dy^{3+} ions from an initial state J to a final ground state J' was calculated using the relation

$$A_{J} = \frac{64\pi^{4}e^{2}}{3h(2J+1)\lambda^{3}} \times \frac{n(n^{2}+2)^{2}}{9} \times \sum_{t=2,4,6} \Omega_{t}(\langle 4f^{N}J \| U^{t} \| 4f^{N}J' \rangle)^{2}. \qquad (4)$$

The total radiative emission probability A_{T} involving all the intermediate terms is given by the sum of the A_{J} terms calculated over all terminal states. Thus, radiative lifetime τ_{rad} of an excited level is given by the inverse of the total radiative emission probability,

$$\tau_{rad} = \frac{1}{\sum_{i} A_{Ji}} = \frac{1}{A_{T}}. \qquad (5)$$

Table 1. Measured and calculated oscillator strengths for Dy^{3+} ions in lead borate glasses. Transitions are from the $^6H_{15/2}$ ground state to the levels indicated. Wavelengths correspond to average transition energies. The three phenomenological intensity parameters Ω_t ($t = 2, 4, 6$) are found to be $\Omega_2 = 4.90 \pm 0.18$, $\Omega_4 = 0.94 \pm 0.19$, $\Omega_6 = 2.07 \pm 0.09$ (in 10^{-20} cm^2 units); $d = \Sigma(P_{meas} - P_{calc}) = 0.7 \times 10^{-6}$.

Levels	Wavelength λ (nm)	Energy ν (cm^{-1})	Oscillator strengths		$P_{meas} - P_{calc}$ ($\times 10^{-6}$)
			P_{meas} ($\times 10^{-6}$)	P_{calc} ($\times 10^{-6}$)	
$^6H_{11/2}$	1695	5 900	1.290	1.375	0.085
$^6F_{11/2}$	1282	7 800	5.730	5.719	0.011
$^6F_{9/2}$	1093	9 150	2.330	2.356	0.026
$^6F_{7/2}$	901	11 100	2.330	2.263	0.067
$^6F_{5/2}$	485	12 430	1.370	1.128	0.242
$^6F_{3/2}$	805	13 300	0.220	0.215	0.005
$^4F_{9/2}$	472	21 200	0.260	0.182	0.078
$^4I_{15/2}$	452	22 100	0.440	0.496	0.056
$^4G_{11/2}$	426	23 450	0.180	0.050	0.130

Table 2. Calculated radiative transition rates A_J, luminescence branching ratios β and corresponding radiative lifetimes τ_{rad} for Dy^{3+} in lead borate glasses. The values of measured lifetime τ_m and quantum efficiency η for the $^4F_{9/2}$ level of Dy^{3+} are also indicated.

Transition	λ (nm)	A_J (s^{-1})	β (%)	τ_{rad} (μs)	τ_m (μs)	η (%)
$^4F_{9/2}-^6F_{1/2}$	1373	0.08	<0.01	638	447	70
$^6F_{3/2}$	1275	0.15	<0.01			
$^6F_{5/2}$	1156	11.05	0.70			
$^6F_{7/2}$	992	6.09	0.40			
$^6H_{5/2}$	918	3.93	0.25			
$^6H_{7/2}$	836	23.61	1.51			
$^6F_{9/2}$	830	9.21	0.60			
$^6F_{11/2}$	749	31.51	2.01			
$^6H_{9/2}$	746	25.29	1.61			
$^6H_{11/2}$	662	99.53	6.35			
$^6H_{13/2}$	573	1046.49	66.75			
$^6H_{15/2}$	480	310.79	19.82			

Figure 2. Luminescence spectra for lead borate glasses with various Dy^{3+} contents.

The luminescence branching ratio β is defined as

$$\beta = \frac{A_J}{\sum_i A_{Ji}} \tag{6}$$

which indicates relative intensities of transitions from the excited level to all terminal levels.

The calculated radiative transition probabilities A_J together with luminescence branching ratios β and corresponding radiative lifetimes τ_{rad} for Dy^{3+} ions in lead borate glasses are summarized in table 2.

3.2. Luminescence

Figure 2 presents luminescence spectra for Dy^{3+} ions in lead borate glasses. Luminescence was analyzed as a function of activator (Dy^{3+}) concentration. Luminescence spectra were recorded under excitation by 386 nm ($^4K_{17/2}$ state) or 450 nm ($^4I_{15/2}$ state) lines. Independently of excitation wavelengths, two relatively intense bands at 480 and 573 nm, and a considerably less intense band at 662 nm, have been observed. They correspond to $^4F_{9/2} \rightarrow ^6H_{15/2}$ (blue), $^4F_{9/2} \rightarrow ^6H_{13/2}$ (yellow) and $^4F_{9/2} \rightarrow ^6H_{11/2}$ (red) transitions of Dy^{3+} ions, respectively. All transitions are shown in the energy level scheme, which was constructed for Dy^{3+} ions in lead borate glass (figure 3). Owing to small energy gaps between all states
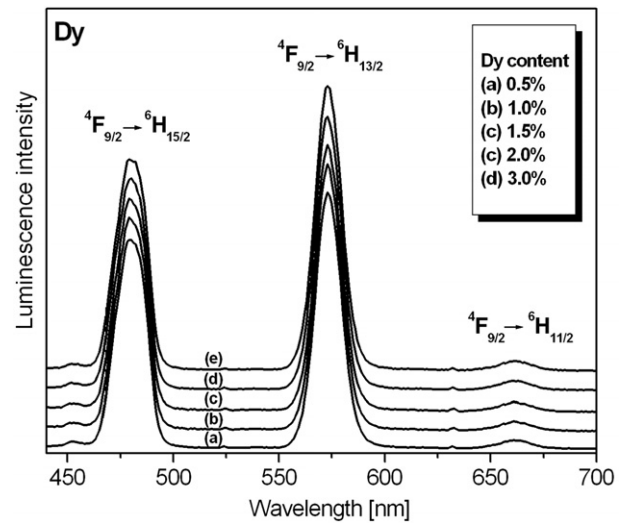
lying above 21 000 cm^{-1}, the $^4F_{9/2}$ state is efficiently populated by non-radiative relaxation. Then, quite strong yellow and blue luminescence originating from the $^4F_{9/2}$ state is observed. This phenomenon is due to large separation ($\sim$6000 cm^{-1}) between the $^4F_{9/2}$ state and the next lower lying $^6F_{1/2}$ state as well as the relatively high phonon energy of the host ($\sim$1300 cm^{-1}).

Several spectral parameters (λ, $\Delta\lambda$, Y/B and τ_m) for Dy^{3+} ions in lead borate glasses were evaluated from the luminescence measurements. The results are given in table 3.

The yellow-to-blue luminescence due to $^4F_{9/2} \rightarrow ^6H_{15/2}$ and $^4F_{9/2} \rightarrow ^6H_{13/2}$ transitions has been analyzed as a function of Dy^{3+} content. The $^4F_{9/2} \rightarrow ^6H_{13/2}$ transition is hypersensitive and its luminescence intensity strongly depends on the host, in comparison to the less sensitive $^4F_{9/2} \rightarrow ^6H_{15/2}$ transition of Dy^{3+}. It results in different yellow-to-blue luminescence intensity ratios (Y/B). The higher values of Y/B indicate the higher degree of covalence between dysprosium and oxygen ions. The intensity of yellow emission due to the $^4F_{9/2} \rightarrow ^6H_{13/2}$ transition increases when the activator concentration varies from 0.5 to 3 wt%. Thus, the yellow-to-blue luminescence intensity ratios (Y/B) are changed from 1.05 to 1.15.
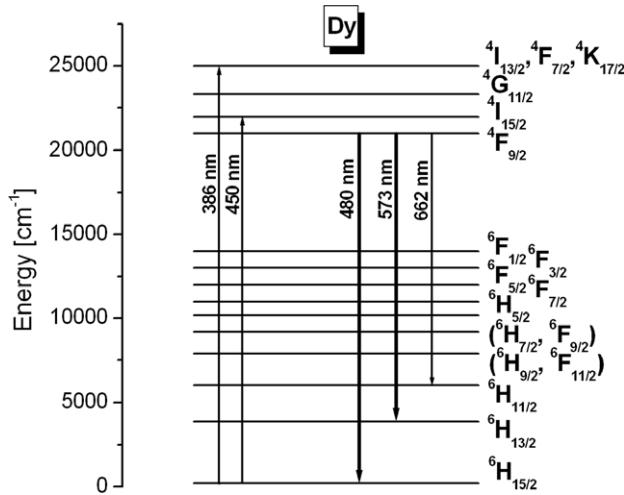
Figure 3. Energy level scheme for Dy^{3+} ions in lead borate glasses. All transitions are also indicated.

Table 3. Spectral parameters (λ, $\Delta\lambda$, Y/B and τ_m) for Dy^{3+} ions in lead borate glasses.

Dy content (wt%)	Transition					
	$^4F_{9/2}$–$^6H_{13/2}$ (yellow)		$^4F_{9/2}$–$^6H_{15/2}$ (blue)			
	λ (nm)	$\Delta\lambda$ (nm)	λ (nm)	$\Delta\lambda$ (nm)	Y/B	τ_m (ms)
0.5	573	14	479	18	1.05	0.47
1.0	573	14	479	18	1.08	0.47
1.5	573	15	480	18	1.11	0.39
2.0	573	14	479	18	1.13	0.36
3.0	573	14	479	18	1.15	0.29

3.3. Luminescence decay analysis

The kinetics of luminescence decays from the $^4F_{9/2}$ state of Dy^{3+} ions in lead borate glasses was investigated. For low Dy^{3+} concentration, the measured $^4F_{9/2}$ lifetime (τ_m) was determined to be 0.47 ms. This is consistent with values of 0.45 and 0.52 ms obtained for borate glasses [65] and crystals [66] containing Dy^{3+} ions. The radiative $^4F_{9/2}$ lifetime (τ_{rad}) calculated from the Judd–Ofelt framework is close to 0.638 ms (see table 2). Thus, the quantum efficiency of the $^4F_{9/2}$ excited state η given by equation (7) is quite large. Its value seems to be close to 70%.

$$\eta = \frac{\tau_m}{\tau_{rad}} \times 100\%. \tag{7}$$

Figure 4 presents luminescence decay curves detected for glass samples with various activator Dy^{3+} content. The luminescence decay curves for the $^4F_{9/2}$ state are changed from a near single exponential to non-exponential with increasing Dy^{3+} content. The measured lifetime for $^4F_{9/2}$ state decreases from 0.47 to 0.29 ms, when Dy^{3+} content varies from 0.5 to 3 wt% (see table 3). This behavior is due to activator–activator interaction increasing. For higher activator concentration, the interaction between neighboring dysprosium ions becomes important and makes a contribution to the energy transfer processes from excited (donor) to ground
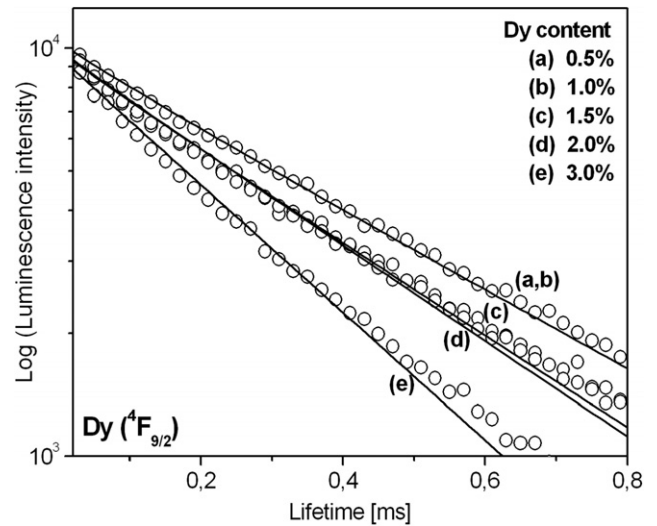

Figure 4. Luminescence decay curves for $^4F_{9/2}$ state of Dy^{3+} ions in lead borate glasses.

(acceptor) Dy^{3+}. This results in concentration-dependent luminescence quenching.

In order to estimate the ion–ion interaction the Inokuti–Hirayama model [64] has been applied for luminescence decay curve analysis. The Inokuti–Hirayama model is applicable only for analysis of energy transfer processes, where the donor–acceptor transfer is faster than migration. Considering a non-exponential character of the decay, the time evolution of the luminescence intensity was fitted to that predicted by the formula:

$$I(t) = A \exp[-(t/\tau_0) - \alpha(t/\tau_0)^{3/s}] \tag{8}$$

where A is a constant, $I(t)$ is the luminescence intensity after pulse excitation, τ_0 is the intrinsic lifetime of the donor in the absence of an acceptor, $s = 6$ for a dipole–dipole interaction between the ions, and α is the parameter given by the relation

$$\alpha = 4/3\pi \Gamma(1 - 3/s) N_a R_0^3 \tag{9}$$

where Γ is the gamma function, N_a is the concentration of acceptor ions and R_0 is the critical transfer distance defined as a donor–acceptor separation for which the rate of energy transfer between a donor and an acceptor is equal to the rate of intrinsic decay τ_0^{-1}.

The donor–acceptor interaction parameter C_{da} and the energy transfer probability W_{da} are calculated using the following relations:

$$C_{da} = R_0^6 \tau_0^{-1} \tag{10}$$

$$W_{da} = C_{da} R_0^{-6}. \tag{11}$$

Results of the fitting procedure using the Inokuti–Hirayama model are given in table 4. The obtained values for the low concentration (0.5 wt%) Dy-doped sample, such as the critical transfer distance $R_0 = 5.78$ Å and donor–acceptor interaction parameter $C_{da} = 0.79 \times 10^{-40}$ cm^6 s^{-1}, are in a good agreement with the results ($R_0 = 5.9$ Å, $C_{da} = 0.80 \times 10^{-40}$ cm^6 s^{-1}) obtained by Jayasankar *et al* [67] for

Table 4. Results of the fitting of the luminescence decay curves from the $^4F_{9/2}$ level of Dy^{3+} ions obtained using the Inokuti–Hirayama model. The molar ion concentrations, the α values, the critical transfer distances, the donor–acceptor interaction parameters and the energy transfer probabilities are reported.

Ln^{3+} (wt%)	N_a (10^{20} ion cm^{-3})	α	R_0 (Å)	C_{da} (10^{-40} cm^6 s^{-1})	W_{da} (s^{-1})
Dy 0.5	0.84	0.12	5.78	0.790	2119
1.0	1.68	0.12	4.58	0.200	2167
1.5	2.52	0.10	3.77	0.070	2438
2.0	3.36	0.06	2.89	0.015	2575
3.0	5.04	0.02	1.75	0.001	3482

fluoroborate glasses doped with Dy^{3+} ions. Additionally, the Inokuti–Hirayama model gives a reasonably good fit for all the samples with Dy^{3+} except the 3.0 wt% Dy-doped sample. The fitting for the 3.0 wt% Dy^{3+} concentration sample shows a small deviation through the whole decay. However, a fit with $s = 8, 10$ applying to the decay curve of 3.0% of Dy^{3+} ions did not find any importance of other multipolar processes. In spite of this fact, it is difficult to exclude the possibility of a migration mechanism presence in higher concentration than 3.0 wt% Dy-doped glass samples. It also results in an unexpectedly smaller value of the critical radius R_0 for the 3.0 wt% Dy-doped glass sample. However, the value of $R_0 = 5.78$ Å for the 0.5 wt% Dy-doped sample is similar to ones (5–5.5 Å) obtained for Pr^{3+} and Tm^{3+} ions in lead borate glasses [68].

The critical transfer distance and measured lifetime were used to calculate the donor–acceptor interaction parameter C_{da} and the energy transfer probability W_{da} given by equations (10) and (11), respectively. Comparison of W_{da} values indicates significantly smaller self-quenching luminescence of Dy^{3+} than Pr^{3+} and Tm^{3+} ions in lead borate glasses [68].

4. Conclusions

Dysprosium-doped lead borate glasses were examined with respect to the experimental measurements and theoretical calculations. Several spectroscopic parameters for Dy^{3+} ions in lead borate glass were determined from absorption and emission measurements and then compared to the theoretical values, which were calculated basing on Judd–Ofelt framework. Luminescence decay curves were well fitted using the Inokuti–Hirayama model and analyzed in order to estimate Dy–Dy interactions in lead borate glass matrix. The luminescence spectra show two bands at 480 and 573 nm, which are related to $^4F_{9/2}$–$^6H_{15/2}$ (blue) and $^4F_{9/2}$–$^6H_{13/2}$ (yellow) transitions of Dy^{3+}. The branching ratio of yellow/blue luminescence and its decay from the $^4F_{9/2}$ state of Dy^{3+} changed with the activator concentration. The systematic studies indicate that Dy-doped lead borate glasses are attractive solid-state laser materials for generation of visible light.

Acknowledgment

References

[1] Balda R, Fernandez J, de Pablos A and Fdez-Navarro J M 1999 *J. Phys.: Condens. Matter* **11** 7411
[2] Qu F and Dantas N O 2003 *Physica* B **327** 79
[3] Wang G, Xu S, Dai S, Yang J, Hu L and Jiang Z 2004 *J. Non-Cryst. Solids* **336** 102
[4] Cascales C, Balda R, Fernandez J, Arriandiaga M A and Fdez-Navarro J M 2006 *J. Non-Cryst. Solids* **352** 2448
[5] Yamauchi H and Ohishi Y 2005 *Opt. Mater.* **27** 679
[6] Song J H, Heo J and Park S H 2003 *J. Appl. Phys.* **93** 9441
[7] Han Y S, Song J H and Heo J 2003 *J. Appl. Phys.* **94** 2817
[8] Courrol L C, Kassab L R P, Fukumoto M E, Wetter N U, Tatumi S H and Morimoto N I 2003 *J. Lumin.* **102/103** 91
[9] Sobczyk M, Starynowicz P, Lisiecki R and Ryba-Romanowski W 2008 *Opt. Mater.* **30** 1571
[10] Balda R, Saez de Ocariz I, Fernandez J, Fdez-Navarro J M and Arriandiaga M 2000 *J. Phys.: Condens. Matter* **12** 10623
[11] Ushida H, Iwadate Y, Hattori T, Nishiyama S, Fukushima K, Ikeda Y, Yamaguchi M, Misawa M, Fukunaga T, Nakazawa T and Jitsukawa S 2004 *J. Alloys Compounds* **377** 167
[12] Pisarski W A, Goryczka T, Wodecka-Duś B, Płońska M and Pisarska J 2005 *Mater. Sci. Eng.* B **122** 94
[13] Ciceo-Lucacel R and Ardelean I 2007 *J. Non-Cryst. Solids* **353** 2020
[14] Xi Y, Xu Z, Hou Z, Liu L, Xu L, Wang W, Affatigato M and Feller S 2002 *Opt. Commun.* **210** 367
[15] Wang M, Liu Q, Liu H and Zhao X 2007 *Opt. Commun.* **274** 218
[16] Saisudha M B and Ramakrishna J 1996 *Phys. Rev.* B **53** 6186
[17] Pisarski W A, Pisarska J, Dominiak-Dzik G, Mączka M and Ryba-Romanowski W 2006 *J. Phys. Chem. Solids* **67** 2452
[18] Ganguli M and Rao K J 1999 *J. Solid State Chem.* **145** 65
[19] Gahlot P S, Seth V P, Agarwal A, Sanghi S, Chand P and Goyal D R 2005 *Physica* B **355** 44
[20] Veerabhadra Rao A, Laxmikanth C, Appa Rao B and Veeraiah N 2006 *J. Phys. Chem. Solids* **67** 2263
[21] Rada S, Culea M, Neumann M and Culea E 2008 *Chem. Phys. Lett.* **460** 196
[22] Pisarski W A, Dominiak-Dzik G, Ryba-Romanowski W and Pisarska J 2008 *J. Alloys Compounds* **451** 220
[23] Pisarska J, Pisarski W A, Dominiak-Dzik G and Ryba-Romanowski W 2006 *J. Mol. Struct.* **792** 201
[24] Malinowski M, Pracka I, Myziak P, Piramidowicz R and Woliński W 1997 *J. Lumin.* **72–74** 224
[25] Tigreat P Y, Doualan J L, Moncorge R and Ferrand B 2001 *J. Lumin.* **94/95** 107
[26] Kaminskii A A, Gruber J B, Bagaev S N, Ueda K, Hommerich U, Seo J T, Temple D, Zandi B, Kornienko A A, Dunina E B, Pavlyuk A A, Klevtsova R F and Kuznetsov F A 2002 *Phys. Rev.* B **65** 125108
[27] Pang M L, Lin J, Wang S B, Yu M, Zhou Y H and Han X M 2003 *J. Phys.: Condens. Matter* **15** 5157
[28] Vazquez R M, Osellame R, Marangoni M, Ramponi R, Diequez E, Ferrari M and Mattarelli M 2004 *J. Phys.: Condens. Matter* **16** 465
[29] Dominiak-Dzik G, Ryba-Romanowski W, Palatnikov M N, Sidorov N V and Kalinnikov V T 2004 *J. Mol. Struct.* **704** 139
[30] Lu X, You Z, Li J, Zhu Z, Jia G, Wang Y, Wu B and Tu Ch 2005 *J. Cryst. Growth* **281** 416
[31] Lu X, You Z, Li J, Zhu Z, Jia G, Wu B and Tu Ch 2005 *J. Phys. Chem. Solids* **66** 1801
[32] Wang H Y, Li J F, Jia G H, You Z Y, Yang F G, Wei Y P, Wang Y, Zhu Z J, Lu X A and Tu C Y 2007 *J. Lumin.* **126** 452
[33] Wang S M, Xiu Z L, Lu M K, Zhang A Y, Zhou Y Y and Yang Z S 2007 *Mater. Sci. Eng.* B **143** 90

[34] Jayasankar C K and Rukmini E 1997 *Physica* B **240** 273
[35] Saisudha M B and Ramakrishna J 2002 *Opt. Mater.* **18** 403
[36] Chandrasekhar A V, Radhapathy A, Reddy B J, Reddy Y P, Ramamoorthy L and Ravikumar R V S S N 2003 *Opt. Mater.* **22** 215
[37] Jayasimhadri M, Moorthy L R, Kojima K, Yamamoto K, Wada N and Wada N 2006 *J. Phys. D: Appl. Phys.* **39** 635
[38] Duan Z, Zhang J and Hu L 2007 *J. Appl. Phys.* **101** 043110
[39] Piramidowicz R, Klimczak M and Malinowski M 2008 *Opt. Mater.* **30** 707
[40] Azeem P A, Balaji S and Reddy R R 2008 *Spectrochim. Acta* A **69** 183
[41] Praveena R, Vijaya R and Jayasankar C K 2008 *Spectrochim. Acta* A **70** 577
[42] Liang X, Zhu C, Yang Y, Yuan S and Chen G 2008 *J. Lumin.* **128** 1162
[43] Tikhomirov V K, Görller-Walrand C and Driesen K 2008 *J. Alloys Compounds* **451** 542
[44] Lakshminarayana G, Qiu J, Brik M G and Kityk I V 2008 *J. Phys.: Condens. Matter* **20** 335106
[45] Lakshminarayana G, Qiu J, Brik M G and Kityk I V 2008 *J. Phys. D: Appl. Phys.* **41** 175106
[46] Lakshminarayana G, Yang H, Teng Y and Qiu J 2009 *J. Lumin.* **129** 59
[47] Tanabe S, Hanada T, Watanabe M, Hayashi T and Soga N 1995 *J. Am. Ceram. Soc.* **78** 2917
[48] Nazabal V, Nemec P, Jedelsky J, Duverger C, Le Person J, Adam J L and Frumar M 2006 *Opt. Mater.* **29** 273
[49] Yang Z, Chen W and Luo L 2005 *J. Non-Cryst. Solids* **351** 2513
[50] Yang Z, Li B, He F, Luo L and Chen W 2008 *J. Non-Cryst. Solids* **354** 1198
[51] Zhao D, Yang G, Xu Y, Zeng H, Nemec P, Frumar M and Chen G 2008 *J. Non-Cryst. Solids* **354** 1294
[52] Rai V K and Rai S B 2004 *Solid State Commun.* **132** 647
[53] Tripathi G, Rai V K and Rai S B 2005 *Spectrochim. Acta* A **62** 1120
[54] Rai V K, Rai S B and Rai D K 2006 *Opt. Commun.* **257** 112
[55] Li A, Lü Q, Zheng Z, Sun L, Wu W, Liu W, Yang Y and Lü T 2007 *J. Appl. Phys.* **102** 113102
[56] Tanabe S, Kang J, Hanada T and Soga N 1998 *J. Non-Cryst. Solids* **239** 170
[57] Srivastava P, Rai S B and Rai D K 2003 *Spectrochim. Acta* A **59** 3303
[58] Mahato K K, Rai A and Rai S B 2005 *Spectrochim. Acta* A **61** 431
[59] Lin H, Pun E Y B, Wang X and Lin X 2005 *J. Alloys Compounds* **390** 197
[60] Lakshminarayana G and Buddhudu S 2006 *Physica* B **373** 100
[61] Lakshminarayana G and Buddhudu S 2007 *Spectrochim. Acta* A **67** 802
[62] Judd B R 1962 *Phys. Rev.* **127** 750
[63] Ofelt G S 1962 *J. Chem. Phys.* **37** 511
[64] Inokuti M and Hirayama F 1965 *J. Chem. Phys.* **43** 1978
[65] Babu P and Jayasankar C K 2000 *Opt. Mater.* **15** 65
[66] Dominiak-Dzik G, Solarz P, Ryba-Romanowski W, Beregi E and Kovács L 2003 *J. Alloys Compounds* **359** 51
[67] Jayasankar C K, Venkatramu V, Surendra Babu S and Babu P 2004 *J. Alloys Compounds* **374** 22
[68] Pisarski W A, Pisarska J, Dominiak-Dzik G and Ryba-Romanowski W 2004 *J. Phys.: Condens. Matter* **16** 6171